2013

Higher-Order Explicit Methods for Laser-Plasma Interactions

J. Paxon Reyes
University of Nebraska-Lincoln

Bradley Allan Shadwick
University of Nebraska-Lincoln, shadwick@unl.edu

Pulsed Power Conference (PPC), 2013 19th IEEE
Year: 2013
Pages: 1 - 5, DOI: 10.1109/PPC.2013.6627594

Higher-Order Explicit Methods for Laser-Plasma Interactions

J. Paxon Reyes and B. A. Shadwick
Department of Physics & Astronomy
University of Nebraska-Lincoln
Lincoln, NE 68588

***Abstract*—The evolution of a short, intense laser pulse propagating in an underdense plasma is of particular interest for laser-plasma accelerator physics and, in some circumstances, is well-modeled by the cold Maxwell-fluid equations. Solving this system using conventional second-order explicit methods in a three-dimensional simulation over experimentally-relevant configurations is prohibitively expensive. This motivated a search for more efficient numerical methods to solve the fluid equations. Explicit methods tend to suffer from stability constraints which couple the maximum allowable time step to the spatial grid size. If the dynamics of the system evolves on a time scale much larger than the constrained time step, an explicit method would require many more update cycles than is physically necessary. In these circumstances implicit methods, which tend to be unconditionally stable, may be attractive. But when physical situations (e.g., Raman processes) need to resolve the fast dynamics, implicit methods are unlikely to exhibit much improvement over explicit methods. Thus, we look for higher-order explicit methods in space that would allow coarser spatial grids and larger time steps. We restrict our discussion to the one-dimensional case and present a comprehensive survey of a wide range of numerical methods to solve the fluid equations, including methods of order two through six in space and two through eight in time. A systematic approach to determine the stability condition is presented using linear stability analysis of numerical dispersion relations. Three higher-order methods are implemented to show their behavior, in terms of numerical stability and energy conservation.**

I. Introduction

The cold Maxwell-fluid equations accurately describe the dynamics involved in laser-plasma acceleration [1]. These equations are often solved numerically using a second-order differencing scheme to approximate the space and time derivatives, leading to a stability-constrained explicit method that tends to be computationally expensive when used in a fully three-dimensional simulation. We shall consider only the one-dimensional fluid equations since the longitudinal dynamics plays the crucial role in shaping the stability constraints. Time t and the propagation direction z are reparameterized by

$$(t,\, z) \mapsto (t,\, \xi = c\,t - z) \tag{1}$$

in order to follow the laser pulse. A consequence of the reparameterization is that the temporal dynamics is effectively slowed down and, since this is not a Lorentz-boosted frame [2], none of the spatial parameters are changed. The laser and plasma wavenumbers k and k_p, respectively, and the laser pulse length L have the same magnitudes as in the lab frame. Thus methods with severe stability constraints can cause large inefficiencies in the time-update calculations due to the temporal step size being tied to the spatial resolution. For example, second-order backwards differencing applied to the 1D fluid equations have the stability constraint $c\,\Delta t/\Delta\xi \lesssim 0.25$, to prevent high-frequency numerical noise from exciting exponentially-growing modes. To maintain acceptable spatial accuracy using second-order methods, a considerable number of grid points per laser wavelength can be required. With only 25 grid points per laser oscillation, the maximum allowable stable time step Δt_M is unnecessarily small by approximately four orders of magnitude (with a laser wavenumber of $k_0 = 10k_p$), and produces an inefficient computer simulation for laser-wakefield accelerator applications.

Implicit methods may entirely relieve the stability constraint and permit reasonable time steps in modeling a forward-traveling laser pulse interacting with a plasma. As an example, an unconditionally-stable implicit method can be formed using second-order midpoint differencing and the resulting simulations maintain the same level of accuracy as in the explicit method except they allow reasonable times steps: depending on the laser wavenumber, the time step can be five or six orders of magnitude larger than the maximum time step Δt_M allowed by the explicit method. This is true as long as the fast dynamics are of little interest. The forward-traveling wave will be nearly stationary in the co-moving coordinate system whereas a backward-traveling wave has an analytical group velocity that is nearly $2c$ in the $+\xi$ direction [3]. With this implicit method, the numerical group velocity of the backward mode is highly sensitive to the size of the time step, dropping by half as the time interval is nominally increased from $\omega_p\Delta t = 0.1$ to $\omega_p\Delta t = 0.2$.

Many physical situations (*e.g.*, Raman processes) require resolving the fast time dynamics for both propagation directions. In such cases, implicit methods are unlikely to exhibit much improvement over explicit methods. But higher-order explicit methods are likely more efficient than the traditional second-order method, allowing for a courser spatial grid and looser coupling between Δt and $\Delta\xi$. We examine a wide range of methods while restricting the discussion to the one-dimensional case. There is no *a priori* way to determine whether a method will work and there are surprisingly many methods that turn out to be unconditionally unstable. We present a systematic approach to determine stability conditions using linear stability analyses of the numerical dispersion relations from these methods. This illustrates how the time step couples with the grid spacing, and we use examples to show how the numerical error of the group velocity depends

978-1-4673-5168-3/13/$31.00 ©2013 IEEE

on the grid size.

II. Linear Stability Analysis

By Lax's theorem [4], [5] we know that only methods which are stable converge to the exact solution for $\Delta t, \Delta\xi \to 0$. Lax's theorem, strictly speaking, only applies to linear equations. However, since the addition of nonlinear dynamics is unlikely to mitigate the effects of a linearly-unstable method, we use the criterion of linear stability in the present analysis.

Written with the reparameterized variables, the one-dimensional cold Maxwell-fluid equations are

$$\begin{aligned}
\left(\frac{\partial^2}{\partial t^2} + 2c\,\frac{\partial^2}{\partial t\,\partial\xi}\right) A_x &= -\frac{4\pi q^2}{m}\,\frac{n}{\gamma}\,A_x\ , \\
\left(\frac{\partial}{\partial t} + c\,\frac{\partial}{\partial\xi}\right) E_z &= -\frac{4\pi q}{m}\,\frac{n}{\gamma}\,p_z\ , \\
\left(\frac{\partial}{\partial t} + c\,\frac{\partial}{\partial\xi}\right) n &= \frac{\partial}{\partial\xi}\left(\frac{n}{\gamma}\,\frac{p_z}{m}\right)\ , \\
\left(\frac{\partial}{\partial t} + c\,\frac{\partial}{\partial\xi}\right) p_z &= mc^2\,\frac{\partial\gamma}{\partial\xi} + qE_z\ ,
\end{aligned} \tag{2}$$

where m is the electron mass, q is electron charge, c is the speed of light, A_x is the transverse vector potential, E_z is the longitudinal electric field, n is the electron plasma density, p_z is longitudinal electron fluid momentum, and $\gamma = \sqrt{1 + q^2A_x^2/m^2c^4 + p_z^2/m^2c^2}$.

The linearized equations admit Fourier modes of the form

$$A_x = \hat{A}_x \mathrm{e}^{i\omega t}\mathrm{e}^{-ik\xi}, \tag{3}$$

where ω and k is the angular frequency and wavenumber in the co-moving coordinate system and $\hat{A}_x$ is the wave amplitude. For the linearized wave equation in system (2),

$$\left(\frac{\partial^2}{\partial t^2} + 2c\,\frac{\partial^2}{\partial t\,\partial\xi}\right) A_x = -\omega_p^2\,A_x\,, \tag{4}$$

the analytical linear dispersion relation is

$$\omega = kc \pm \sqrt{k^2c^2 + \omega_p^2}\,, \tag{5}$$

where $\omega_p = k_p c$ is the plasma frequency. If the imaginary part of ω is negative, the time exponential term of (3) would consist of an oscillating $\exp\left[i\mathrm{Re}(\omega)t\right]$ and an exponentially-growing $\exp\left[-\mathrm{Im}(\omega)t\right]$ factor. The condition for numerical instability is analogous to the presence of this growing exponential.

Discretizing (4) in space, the system is treated as a set of ODEs in time (*i.e.,* using the method of lines [7]):

$$\dot{\mathbf{y}} = A\,\mathbf{y} \tag{6}$$

where

$$\mathbf{y} = \begin{pmatrix} A_x \\ \dot{A}_x \end{pmatrix} \quad \text{and} \quad A = \begin{pmatrix} 0 & 1 \\ -\omega_p^2 & -2c\,\theta \end{pmatrix}, \tag{7}$$

with θ the discrete Fourier transform of the spatial difference operator (see the first column of Table I). Let $\mathbf{y}^n$ be the numerical approximation of $\mathbf{y}$ at time $t = n\,\Delta t$. Then

$$\mathbf{y}^{n+1} = M\,\mathbf{y}^n, \tag{8}$$

where the update matrix

$$M = \sum_{l=0}^{N} \frac{\Delta t^l}{l!}\,A^l \tag{9}$$

depends on the order N of the temporal accuracy. The numerical dispersion relation $\Omega(\kappa)$ is related to the eigenvalues, λ, of M by

$$\mathrm{e}^{i\Omega(\kappa)} = \lambda\ , \tag{10}$$

where the numerical angular frequency $\Omega = \omega\,\Delta t$ and the numerical wavenumber $\kappa = k\,\Delta\xi$.

Analogous to (3), discrete Fourier modes have the form

$$(A_x)_j^n = \hat{A}_x\,\mathrm{e}^{in\Omega}\mathrm{e}^{-ij\kappa} \tag{11}$$

and, as in the analytical case, if the imaginary part of the numerical dispersion relation $\Omega(\kappa)$ is negative over any range in κ, the numerical solution will exhibit an instability with numerical growth rate $\Gamma = -\mathrm{Im}\,\Omega$. Typically, $\mathrm{Im}\,\Omega$ is negative over a finite interval in κ corresponding to a range of Fourier modes in k (given a particular $\Delta\xi$). Although initial parameters in a simulation may stay well clear of these growing modes, rounding errors and numerical noise tend to excite higher-order modes. With sufficient time propagation in the simulation, these growing modes will dominate all others. Therefore, if a method leads to $\mathrm{Im}\,\Omega < 0$ at any point, it is said to be unstable.

Table I contains a summary of the stability analysis for the higher-order methods examined. In the $\omega_p = 0$ vacuum case, all occurrences of the intervals Δt and $\Delta\xi$ expressed in the eigenvalues of M appear as the ratio $r = c\,\Delta t/\Delta\xi$, which is thus a suitable quantity to describe the stability constraint. Though the eigenvalues do have a dependence on $\Delta\xi$ when the linear plasma is considered, the dependence is not substantial and has little effect on the stability constraint. Still, this means the values listed in the table are accurate approximations but not exact. A particular value of $\Delta\xi$ based on the spatial resolution requirements would have to be specified for a particular situation to find the precise stability constraint. Since the numerical dispersion relation $\Omega(\kappa)$ is 2π-periodic in κ and symmetric about $\kappa = \pi$, only the domain from 0 to π needs to be considered, which corresponds to Fourier modes of k/k_p between 0 and 125, using $\Delta\xi = 0.025$.

III. Numerical Analyses

A number of methods will be analyzed in more detail: the traditional second-order backward method and, with time order $N = 4$, central differencing methods of order two, four, and six. The analyses will use the grid spacing $\Delta\xi = 0.025/k_p$ such that 25 grid steps are used to sample one oscillation of the laser with wavenumber $k_0 = 10k_p$.

Accuracy of the numerical method can be inferred by comparing the analytical v_g^{a} and numerical v_g^{n} group velocities. As seen from the analytical dispersion relation (5) in the co-moving coordinate system, with k-modes around $10k_p$, a forward-traveling laser pulse will have a small group velocity while a backward-traveling pulse approaches a group velocity of $2c$. Thus, it is expected that the "slower" forward-traveling modes will have less numerical artifacts compared

TABLE I. MAXIMUM STABLE VALUES OF $c\Delta t/\Delta\xi$ FOR A GIVEN SPATIAL DIFFERENCING SCHEME IN ξ. 'US' DENOTES METHODS THAT ARE UNCONDITIONALLY UNSTABLE. SEE REF. [6].

	Spatial Discretization	Temporal Order 2	3	4	5	8
2nd	$f' = \frac{1}{2\delta}(3f_j - 4f_{j-1} + f_{j-2})$	0.25	0.3	0.35		
	$f' = \frac{1}{2\delta}(f_{j+1} - f_{j-1})$	US	0.8	1.4		
3rd	$f' = \frac{1}{6\delta}(11f_j - 18f_{j-1} + 9f_{j-2} - 2f_{j-3})$	US	US	US		
	$f' = \frac{1}{6\delta}(3f_j - 6f_{j-1} + f_{j-2} + 2f_{j+1})$	0.48	0.8	0.85		
4th	$f' = \frac{1}{12\delta}(25f_j - 48f_{j-1} + 36f_{j-2} - 16f_{j-3} + 3f_{j-4})$	US	US	US		
	$f' = \frac{1}{12\delta}(-8f_{j-1} + 8f_{j+1} + f_{j-2} - f_{j+2})$	US	0.63	1.05		
	$f' = \frac{1}{12\delta}(10f_j - 18f_{j-1} + 6f_{j-2} - f_{j-3} + 3f_{j+1})$	US	0.45	0.55	0.59	
5th	$f' = \frac{1}{60\delta}(137f_j - 300f_{j-1} + 300f_{j-2} - 200f_{j-3} + 75f_{j-4} - 12f_{j-5})$	US	US	US		
	$f' = \frac{1}{60\delta}(20f_j - 60f_{j-1} + 15f_{j-2} - 2f_{j-3} + 30f_{j+1} - 3f_{j+2})$	0.09	0.72	0.85		
6th	$f' = \frac{1}{60\delta}(45f_{j+1} - 45f_{j-1} - 9f_{j+2} + 9f_{j-2} + f_{j+3} - f_{j-3})$	US	0.55	0.87	US	1.05

to backward-traveling modes for all stable methods. The numerical group velocity can be expressed as

$$\frac{v_g^{\mathrm{n}}}{c} = \left(\frac{1}{c}\frac{\Delta\xi}{\Delta t}\right)\frac{\partial(\omega\Delta t)}{\partial(k\Delta\xi)} = \frac{1}{r}\frac{\partial\Omega}{\partial\kappa}\ , \tag{12}$$

and the v_g^{n} of the four numerical methods will be compared against each other and with v_g^{a}.

A shorthand notation is adopted to simplify the description of the following methods by listing the spatial ordering and the differencing scheme (*i.e.,* backward or central) followed by the temporal order (*e.g.,* "2t" for second-order in time). The traditional method using second-order backwards differencing in space and second-order time approximation is written as "2b2t."

A. Stability Considerations

We examine solutions of the numerical dispersion relation for various spatial differencing schemes and temporal integration orders.

1) Second-Order Backward Differencing in Space (2b2t): As stated before, the traditionally used method to solve system (2) uses backwards differencing in space. The imaginary part of Ω of the forward-traveling mode (Fig. 1a) is strictly positive for a range of r. This is in contrast to the backward-traveling mode (Fig. 1b) where, for $r > 0.25$, there is a range of k where $\mathrm{Im}\,\Omega < 0$. Only by keeping $r \leq 0.25$ will the numerical instability be completely avoided.

An example of an unconditionally-unstable method can be made by replacing the backward spatial differencing of 2b2t with a central differencing of the same order. The results is that, for all k and r in both the forward and backward waves, the imaginary part of $\mathrm{Im}\,\Omega \leq 0$. In this case, all modes grow exponentially in time.

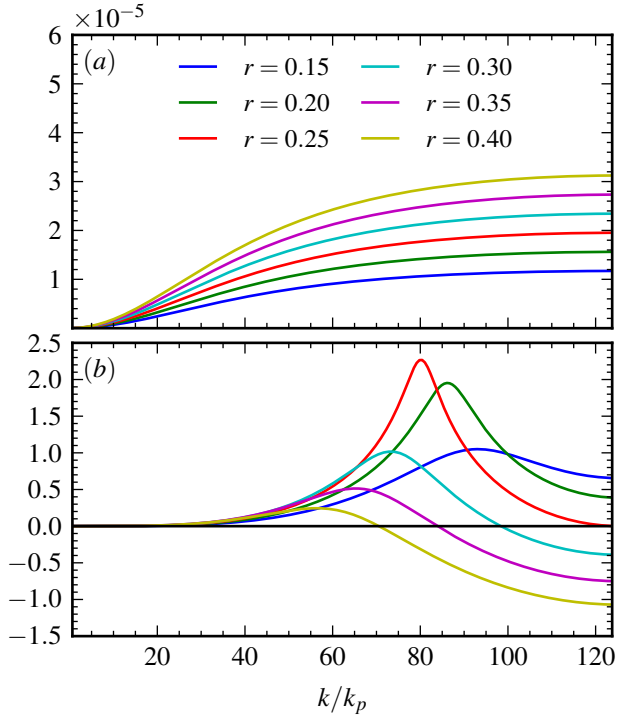

Fig. 1. $\mathrm{Im}\,\Omega$ using second-order backwards differencing plotted against k with $\Delta\xi = 0.025/k_p$ and $N = 2$. (a) The forward mode $\mathrm{Im}\,\Omega$ is fairly insensitive to r with numerical dissipation on the order of 10^{-5}. (b) The backward mode $\mathrm{Im}\,\Omega$, on the other hand, has much more variation in r. The criterion for stability is $r \leq 0.25$, although significant numerical dissipation exists compared to that of the forward mode.

2) Second-Order Central Differencing in Space (2c4t): Surprisingly, going to order four for the time approximation while keeping the previously-mentioned second-order central differencing in space produces the most efficient numerical

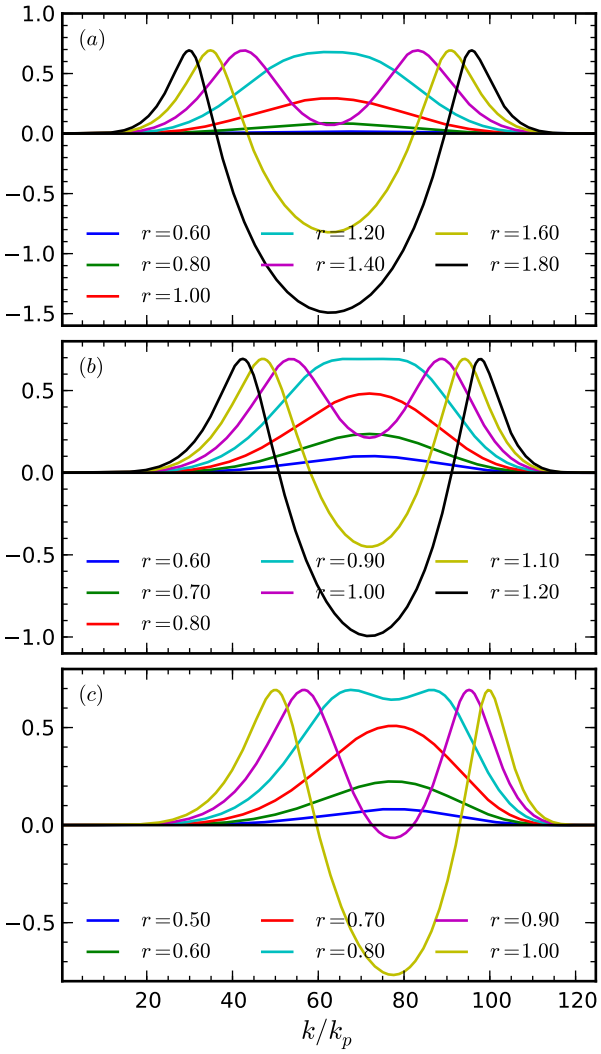

Fig. 2. $\mathrm{Im}\,\Omega$ for methods using central differencing: (a) the 2c4t method; (b) the 4c4t method; and (c) the 6c4t method. In all cases only the backwards mode is shown; the forwards mode $\mathrm{Im}\,\Omega \lesssim 10^{-12}$ and is insensitive to both r and κ.

method (2c4t). For the forward mode, $\mathrm{Im}\,\Omega$ is nearly zero for all k and r; thus the numerical dissipation is negligible for these modes. The backward modes of this method (see Fig. 2a) show less dissipation compared to the 2b2t method.

3) Fourth-Order Central Differencing in Space (4c4t): Here the imaginary part of the forward mode Ω is essentially zero. Otherwise, in terms of the stability conditions and the magnitude of the numerical dissipation, there is no improvement by applying the fourth-order central differencing in space to a fourth-order accurate temporal method. As seen from Fig. 2a and Fig. 2b, for comparable values of r, the level of dissipation with $2c4t$ is much less than with $4c4t$. Of course, with higher-order approximations we do expect the numerical accuracy behave to better for larger ranges of k and also to exhibit faster convergence. Faster convergence of the total energy error will be shown in the next sectio45n.

4) Sixth-Order Central Differencing in Space (6c4t): The highest spatial order we illustrate is the sixth-order central. Again, for the forward mode $\mathrm{Im}\,\Omega$ essentially zero. For the

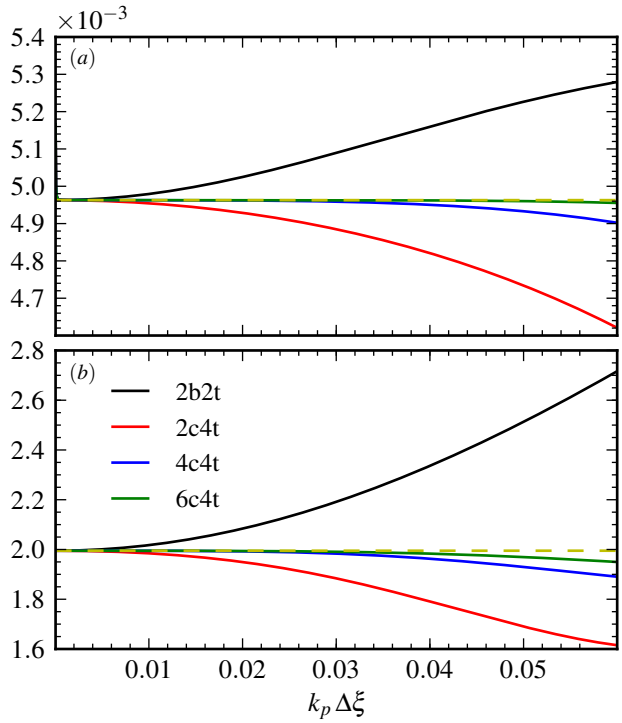

Fig. 3. Numerical group velocities of: (a) the forward and (b) backward modes, in units of c.

backward mode, the $\mathrm{Im}\,\Omega$ shows features similar to $2c4t$ and $4c4t$. In general, the maxima and minima have shifted toward higher k and the maximum r is reduced compared to the other fourth-order time methods.

Higher-order time approximations, like the method from Table I using eighth-order time and sixth-order central differencing, may lead to a significantly large value of r (1.05 in this case) but the extra work required for such high-order time calculations is not desirable when the time steps are already constrained to be far smaller than is required for accuracy.

B. Accuracy Considerations

The analytical group velocity for the linear wave equation (4), using (5), is

$$\frac{v_g^{\mathrm{a}}}{c} = 1 \pm \frac{k^2c^2}{\sqrt{k^2c^2+\omega_p^2}} \tag{13}$$

and depends only on the wavenumber k, whereas the numerical group velocity (12) also has dependencies on the numerical parameters r and $\Delta\xi$ and on the differencing scheme. The Δt dependence enters through r. For the methods discussed above, the numerical group velocities have been plotted in Fig. 3, along with the analytical group velocity (broken yellow line), as a function of the parameter $\Delta\xi$ for a chosen wavenumber $k = 10k_p$. The values of r were chosen based on Table I but adjusted to allow even subintervals of time and space in computer simulations. Specifically the r used were 0.25, $4.0/3.0$, 1.0, and 0.80 for methods 2b2t, 2c4t, 4c4t, and 6c4t, respectively. Since r was fixed, Δt and $\Delta\xi$ varied dependently. The forward mode Fig. 3a and backward mode Fig. 3b group velocities are physically accurate for small $\Delta\xi$ and then depart

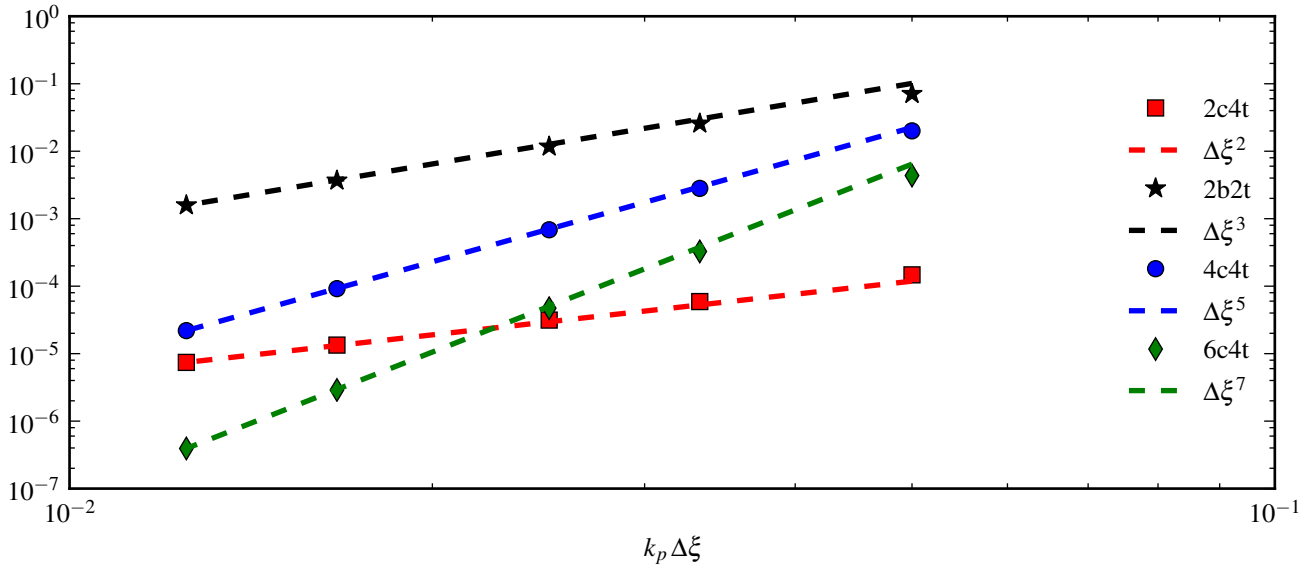

Fig. 4. Relative error of the total system energy after a time propagation of $50/\omega_p$ *versus* grid size $\Delta\xi$. The order of the spatial differencing corresponds to the behavior of the energy error scaling. The broken lines indicate power law scalings associated with the spatial orderings.

from the analytical group velocity at large $\Delta\xi$. For larger wavenumbers, significant departures occur at smaller $\Delta\xi$.

The nonlinear system (2) is energy conservative [8], so tracking the change in the total system energy is a convenient way to assess a method's quality. All four methods were implemented in a fully-nonlinear, one-dimensional code. The total energy includes contributions from the laser, the plasma wakefield, and the particles. After a propagation time of $T = 50/\omega_p$ the total energy was calculated and compared with the initial energy, taking the absolute value of the difference and scaling by the initial energy. The r parameters were the same as in Fig. 3, and the initial shape of the laser pulse was a Gaussian with average wavenumber $k = 10k_p$, width $k_pL = 2$, and amplitude $A_0 = mc^2/q$. Fig. 4 shows the relative energy error as a function of the spatial grid size $\Delta\xi$. Using larger $\Delta\xi$ in space leads to greater energy errors, in general.

IV. Conclusion

We have analyzed all practical higher-order explicit methods for laser-plasma interactions using the cold Maxwell-fluid equations. In terms of the most relaxed stability constraints and ease of calculation, the 2c4t explicit method was found to be the most efficient among those analyzed. In comparison, the largest time step with this method is over five times larger than is possible with the traditional 2b2t method while the numerical dissipation per time step is also significantly less. Thus, the overall effective dissipation for 2b2t is greater by a factor of approximately five over the 2c4t method.

The numerical group velocities are sensitive to the grid spacing. As expected, higher-order spatial methods are accurate for a wider range of $\Delta\xi$. Extremely high temporal resolutions are mandated by the stability constraints. Even for simulations using the largest stable time steps, the energy error only depends on $\Delta\xi$. The energy behavior of these explicit methods are predictable, obeying expected power laws based on the accuracy of the spatial order.

These one-dimensional numerical methods are suitable for higher-dimensional simulations. The addition of transverse dimensions may alter the time constraints but they do not drastically affect a method's stability. So, if resolving fast dynamics are of interest, high-order explicit methods are an attractive option.

Acknowledgments

The authors gratefully acknowledge useful discussions with G. M. Tarkenton and C. B. Schroeder. This work was supported by the U. S. Department of Energy under Contract Nos. DE-FG02-08ER55000 and DE-SC0008382 and by the National Science Foundation under Contract No. PHY-1104683.

References

[1] E. Esarey, C. B. Schroeder, and W. P. Leemans, "Physics of laser-driven plasma-based electron accelerators," *Reviews of Modern Physics*, vol. 81, no. 3, pp. 1229–1285, 2009.

[2] J.-L. Vay, C. G. R. Geddes, E. Cormier-Michel, and D. P. Grote, "Effects of hyperbolic rotation in minkowski space on the modeling of plasma accelerators in a Lorentz boosted frame," *Phys. Plasmas*, vol. 18, no. 3, p. 030701, 2011.

[3] J. P. Reyes and B. A. Shadwick, "An unconditionally-stable numerical method for laser-plasma interactions," in *Advanced Accelerator Concepts: Proceedings of the 15th Advanced Accelerator Concepts Workshop*, ser. AIP Conference Proceedings, R. Zgadzaj and E. Gaul, Eds., vol. 1507. AIP, 2013, pp. 939–944.

[4] R. Richtmyer and K. W. Morton, *Difference Methods for Initial Value Problems*. Wiley-Interscience, 1967.

[5] J. W. Thomas, *Numerical Partial Differential Equations: Finite Difference Methods*, ser. Texts in Applied Mathematics, Vol. 22. Springer, 1995.

[6] G. M. Tarkenton, B. A. Shadwick, and C. B. Schroeder, "Higher-order differencing schemes for modeling intense laser-plasma interactions," *Bull. Am. Phys. Soc.*, vol. 48, no. 7, p. 108, 2003.

[7] W. E. Schiesser, *The Numerical Method of Lines: Integration of Partial Differential Equations*. San Diego: Academic Press, 1991.

[8] B. A. Shadwick, C. B. Schroeder, and E. Esarey, "Nonlinear laser energy depletion in laser-plasma accelerators," *Phys. Plasmas*, vol. 16, no. 5, p. 056704, 2009.